Published online 1 February 2013 *Nucleic Acids Research, 2013, Vol. 41, No. 5* ***3173–3189***
doi:10.1093/nar/gkt051

MRX protects fork integrity at protein–DNA barriers, and its absence causes checkpoint activation dependent on chromatin context

Iben B. Bentsen[1], Ida Nielsen[1], Michael Lisby[2], Helena B. Nielsen[1], Souvik Sen Gupta[1], Kamilla Mundbjerg[1], Anni H. Andersen[1] and Lotte Bjergbaek[1,*]

[1]Department of Molecular Biology and Genetics, University of Aarhus, Aarhus 8000, Denmark and [2]Department of Biology, University of Copenhagen, Copenhagen 2200, Denmark

Received October 12, 2012; Revised January 3, 2013; Accepted January 10, 2013

ABSTRACT

To address how eukaryotic replication forks respond to fork stalling caused by strong non-covalent protein–DNA barriers, we engineered the controllable Fob-block system in *Saccharomyces cerevisiae*. This system allows us to strongly induce and control replication fork barriers (RFB) at their natural location within the rDNA. We discover a pivotal role for the MRX (Mre11, Rad50, Xrs2) complex for fork integrity at RFBs, which differs from its acknowledged function in double-strand break processing. Consequently, in the absence of the MRX complex, single-stranded DNA (ssDNA) accumulates at the rDNA. Based on this, we propose a model where the MRX complex specifically protects stalled forks at protein–DNA barriers, and its absence leads to processing resulting in ssDNA. To our surprise, this ssDNA does not trigger a checkpoint response. Intriguingly, however, placing RFBs ectopically on chromosome VI provokes a strong Rad53 checkpoint activation in the absence of Mre11. We demonstrate that proper checkpoint signalling within the rDNA is restored on deletion of *SIR2*. This suggests the surprising and novel concept that chromatin is an important player in checkpoint signalling.

INTRODUCTION

The path of a replication fork is loaded with obstacles, which impose a frequent threat for the replication fork and make the process of DNA replication fragile. These obstacles are mainly caused by exogenous agents or reactive metabolic products that inevitably damage the DNA. In addition, particular regions in the genome, such as replication slow zones, constitute a challenge to replication fork movement and are associated with a high incidence of chromosomal rearrangements (1,2). Natural replication-impeding sequences also exist, which may form tight protein–DNA complexes that potentially inhibit fork progression (3,4). Replication fork arrest is often temporary, and if the fork is stabilized during this event, DNA synthesis can resume after the obstacle is removed. However, if cells are unable to resume replication, the arrest becomes irreversible, and fork collapse may occur. Recombination may then be a necessary outcome for the cell. Appropriate cellular responses to stalled replication forks are thus essential both for efficient DNA synthesis and the maintenance of genomic stability.

The cellular responses to fork stalling in eukaryotes have been most intensively studied using genotoxic drugs, but recently, more focus has been dedicated to study the cellular response to natural existing replication fork barriers (RFB). Of these, the best studied are the RFB found in the rDNA locus in *Saccharomyces cerevisiae*, which on binding of the Fob1 protein constitutes a strong protein–DNA barrier (5,6), and the replication termination sequence 1 (RTS1) barrier in *S. pombe*, which generates unidirectional replication at the mating-type locus (7).

The cellular response to replication fork stalling caused by naturally existing RFBs may differ in many aspects from the response to genotoxic drugs such as hydroxurea (HU). In the latter case, it is important to maintain a coupling between DNA helicase activity and polymerase activity to avoid extensive DNA unwinding and thereby generation of single-stranded DNA (ssDNA) exposure ahead of the stall site (8). Physical barriers, which hinder helicase movement, will not have to cope with this

*To whom correspondence should be addressed. Tel: +45 87156315; Fax: +45 154902; Email: lbj@mb.au.dk
Present address:
Helena B. Nielsen, Department of Biology, University of Copenhagen, Copenhagen 2200, Denmark.
Kamilla Mundbjerg, Department of Molecular Medicine, Aarhus University Hospital, Aarhus 8000, Denmark.

problem, but replisome stabilization is still essential during stalling. This could require a functional checkpoint as seen for replisome resumption after methyl methane sulphonate (MMS) or HU exposure (9–13). However, experiments with ectopically placed RFBs in *S. cerevisiae* disclose a checkpoint independent pausing and recovery of the replisome at these barriers, contrasting the regulation of HU-stalled forks (14). A similar study from *S. pombe* reveals that cell viability in the presence of inducible RTS1 barriers does not require checkpoint kinases, but opposed to the former study, stalling rapidly leads to replisome disassembly (15).

Recombination is often associated with stalled replication forks. Although unscheduled recombination is undesirable, there is accumulating evidence that homologous recombination (HR) does play crucial roles in the rescue of stalled replication forks both in *E. coli* and in eukaryotic cells (15–18). Recently, rescue of a disassembled fork at the RTS1 barrier in *S. pombe* was suggested to occur via a double-strand break (DSB) independent but recombination dependent pathway through template switching, which leads to chromosomal rearrangements (19,20). In contrast, replication fork stalling at an ectopically placed RFB in *S. cerevisiae* has been suggested to be stably maintained in a recombination independent way (14). These discrepancies may reflect different evolutionary choices between organisms and thus highlight the importance of further investigations to dissect the cellular response to roadblocks and to better understand the relation between stalled forks, checkpoint and recombination events.

The rDNA constitutes a perfect *in vivo* model system for analysing replication fork stalling, as this is a natural event, taking place during each cell cycle in this compartment. Furthermore, the unidirectional mode of DNA replication and the repetitive nature of the rDNA add a strong pressure on the active replication fork, and thus, identification of factors involved in replication fork integrity may prove easier using the rDNA as a model system. To analyse the cellular response to replication fork stalling, we therefore took advantage of the rDNA and engineered a cellular system in *S. cerevisiae*, which allows us to strongly induce and control the barriers at this location. Using this Fob-block system, we uncover a pivotal role for the MRX complex at RFBs, which differs from its acknowledged role in DSB processing. Moreover, our studies reveal the unprecedented concept that chromatin context influences checkpoint activation.

MATERIALS AND METHODS

Yeast strains and plasmids

Strains used were constructed using standard genetic techniques and are listed in Supplementary Table S1. All strains are derivatives of the original W303 genetic background with a mutation in *RAD5*. We therefore confirmed that the growth defect observed for *mre11Δ* on galactose was not due to a non-functional *RAD5* (data not shown). All deletions of *MRE11*, *XRS2* and *RAD50* were tested for MMS sensitivity, as these strains very easily obtained suppressors, which gave rise to MMS resistance (data not shown).

To generate yeast strains with RFBs inserted ectopically at chromosome VI, we modified pFA6a-based plasmids in the following way. The RFB sequence was generated by polymerase chain reaction (PCR) on genomic DNA using primers LBo-81 and LBo-82, respectively. The PCR product obtained was cloned into pFA6a-KanMX4 using *Avr*II and *Spe*I cloning sites, ligation was done in the presence of the enzyme and positive colonies were verified by sequencing (KanMX6-3xRFB, pLB112). To obtain strains with eRBF, the PCR product obtained with primer LBo-50 and LBo-117 on pLB112 was used for homologous recombination-mediated integration of 3xRFB close to *ARS607* in a non-transcibed region between *ATG18* and *ROG3*. Plasmid pML38 for integrating the *tetO* array into the intergenic region iYFR020W is described in (21). Plasmids and primers are listed in Supplementary Table S2 and S3, respectively.

Yeast growth

Cells were grown at 30°C in YP medium supplemented with 2% raffinose (YPRaff), if not otherwise stated. Overnight cultures were diluted and grown for two generations before cells were synchronized in the G1 phase of the cell cycle by the alpha-factor mating-type pheromone (Lipal Biochem, Switzerland) in YPRaff (pH 3.5) for 90 min. Induction of the *FOB1* gene was carried out in G1-arrested cells for 90 min in YPRaff supplemented with 3% galactose (pH. 3.5) before cells were washed several times and released into S phase in YPRaff supplemented with 3% galactose.

Protein expression

Yeast strain LBy-365 was grown overnight in YPRaff medium at 30°C. Culture was diluted and grown to a log phase culture of 1×10^7 cells/ml, before it was divided into two cultures. Two percent galactose was added to one of the cultures. Aliquots were taken from each culture at the indicated times. Trichloroacetic acid precipitation of proteins were performed, sodium dodecyl sulphate–polyacrylamide gel electrophoresis (10% gels) conducted and western blotting carried out using monoclonal antibody against GST (Santa Cruz) and Mcm2 (Santa Cruz).

Spot assays

Cells were grown in liquid YPRaff O/N, adjusted to $OD_{600} = 1$ and 10-fold serial dilutions spotted on YPD and YP + 3% galactose plates, respectively. Plates were incubated for 2 days at 30°C.

Fluorescence-activated cell sorting

Samples were taken for fluorescence-activated cell sorting (FACS) analysis during the various experiments and processed as described in (22). Samples were analysed in a BD FACSCalibur.

2D DNA gels

Cells were grown at 20°C. Yeast genomic DNA was isolated from 2×10^9 cells by using Genomic-tip 20/G (QIAGEN) as described in (23). After the digestion with restriction enzymes (*Bgl*II for the rDNA), the DNA was subjected to neutral/neutral 2D gel analysis as described in (24). Southern blotting was carried out using probes with primers indicated in Supplementary Table S3 and shown in Figure 1A. Image analysis was performed using the Quantity One software. Replication fork stalling was quantified by calculating the percentage of the specific replication fork stalling signal relative to the 1 N spot followed by normalization to the values to time point 0.

DSB assay

Isolation of intact yeast DNA was basically performed as described previously with few modifications (25). Briefly, 9×10^7 cells/plug were used. Cells were re-suspended in 50 µl of cold buffer [0.1 M ethylenediaminetetraacetic acid (EDTA), pH 8, 0.01 M Tris, pH 7.6, and 0.02 M NaCl] containing 5 µl of zymolase (zymolase-20T *Arthrobacter luteus*, 20 000 U/gm) at a stock concentration of 20 mg/ml. The suspension was warmed for 42°C for 10 s and mixed briefly with 50 µl of 1% low melting agarose. Digestion was carried out with *Bgl*II (60 units). Gel plugs were loaded into wells of a 1% agarose gel, which was run in TBE at 2 V/cm at 4°C for 20 h. Standard Southern blotting was carried out.

Pulsed field gel electrophoresis

All steps for pulsed field gel electrophoresis were performed as described in (25). Southern blotting was carried out using a probe for Chr. XII, and for Chr. II, primers for these probes are indicated in Supplementary Table S3. Quantification of the amount of Chr. XII and Chr. II entering the gel was performed using Quantity One software, and shown is an average of two experiments performed. The intensity of the signals at the different time points is calculated relative to timepoint 0, which is set to 1.

Chromatin immunoprecipitation

In all, 50 ml of cells (2×10^7 cells/ml) were cross-linked with 1% formaldehyde for 15 min at 25°C. Glycine was added to a final concentration of 125 mM, and the incubation continued for 5 min. Cells were harvested and washed with 1 ml PBS (137 mM NaCl, 2.7 mM KCl, 1.5 mM KH_2PO_4, 8 mM $Na_2HPO_42 \cdot H_2O$, pH 7). Chromatin immunoprecipitation (ChIP) was performed using polyclonal antibody against RPA (RFA1) (Agrisera, AS07 214). Antibody was bound to Dynabeads M-280 (Invitrogen Dynal AS, Norway) (5 µl/sample). Dynabeads without antibody were used as background control. The cell samples were added to 700 µl of lysisbuffer (140 mM NaCl, 1 mM EDTA, 1% triton-x-100, 50 mM hepes, pH 7.5, protease inhibitors: 0.2 mM PMSF, 1 mM benzamidine, 0.5 µg/ml of leupeptin, 20 µM antipain, 1 µg/ml of pepstatin A, 100 µg/ml of TLCK, 100 µg/ml of TPCK) and acid-washed glass beads before they were lysed using a ribolyser (Hybaid Ltd.). The samples were enriched for chromatin-bound protein by centrifugation at 13 000 r.p.m. in 15 min. In all, 1 ml of lysis buffer was added to the DNA with the bound proteins before the DNA was sonicated to give fragments of ~500–1000 bp. The extract was split into two tubes either containing antibody coupled Dynabeads or Dynabeads alone (control) and incubated at 4°C for 2 h. Afterwards, the beads were washed twice with lysis buffer, once with wash buffer (500 mM NaCl, 1 mM EDTA, 0.5% NP-40, 10 mM Tris, pH 8, protease inhibitors as in the lysis buffer) and once with TE buffer. The interactions between antibodies and beads were reversed by addition of TE + 1% SDS and incubation at 65°C for 10 min. Samples were incubated at 65°C overnight in TE + 1% SDS. Next day, the samples were proteinase K digested for 2 h at 37°C before LiCl was added and phenol-chloroform extraction performed. The recovered DNA was amplified with real-time PCR using a Stratagene MX3000 and performed with 5× AHPolHS EvaGreen qPCR Mix Plus (AH zymes). ChIP data were averaged for three independent experiments with real-time PCR performed in duplicate. Error bars are standard deviations. Fold increase is calculated as the amount of protein bound to Dynabeads (Ip) with antibody compared with the amount of protein bound to Dynabeads alone (Beads): Fold increase = $2^{(\text{CT Input} - \text{CT Ip})/2^{(\text{CT Input} - \text{CT Beads})}}$. The height of the bars in the figure represents fold increase relative to time point 0. Sequences of primers used can be found in Supplementary Table S3.

Rad53 *in situ* kinase assay

All steps of the *in situ* kinase assay (ISA) are as described in (26), except that 5 µCi/ml of [γ-^{32}P] adenosine triphosphate was used. For every sample, protein concentration was determined by Comassie blue before equal loading on 10% SDS–polyacrylamide gels along with 5 µl of a standard (MMS ctrl) containing a known amount of MMS activated Rad53p. Dried filters were exposed to a Typhorn Trio+. After exposure, filters were re-probed with goat anti-Mcm2 (Santa Cruz) to check loading and to allow comparison among different gels and mutants. Experiments were performed 2–3 times with similar results.

RESULTS

Generation of a controllable Fob-block system with inducible RFBs in the rDNA

To address how eukaryotic replication forks respond to fork stalling caused by strong non-covalent protein–DNA barriers, we engineered a controllable Fob-block system in *S. cerevisiae*, which take advantage of the rDNA as a model system. We generated a yeast strain with expression of the *FOB1* gene under control of the *GAL1,10* promoter. Induction of *FOB1* generates high levels of active RFBs in the rDNA and causes unidirectional replication at this locus owing to stalling of leftward moving forks (Figure 1A). This strain is referred to as *GAL-FOB1*.

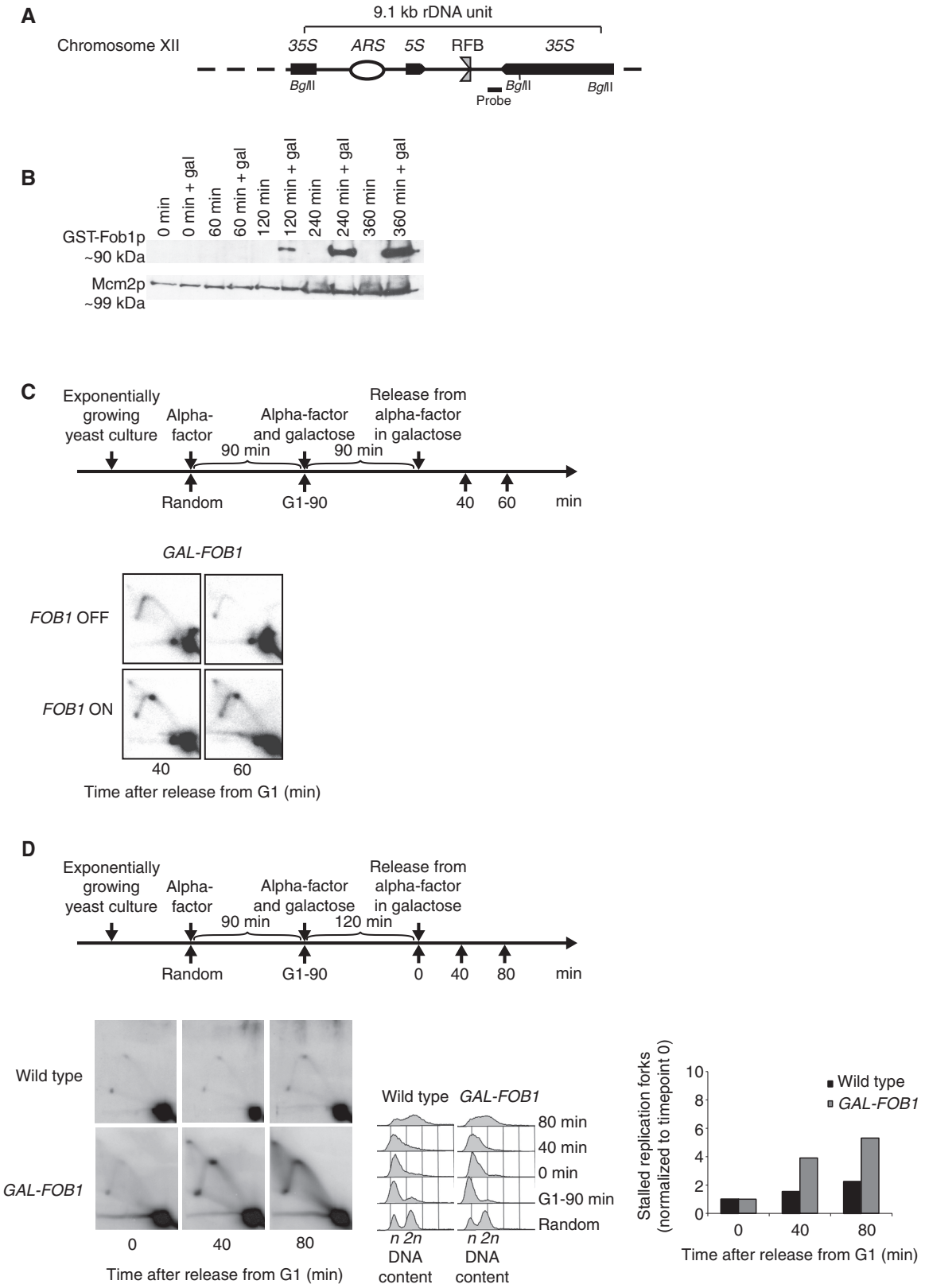

Figure 1. Verification of the Fob-block system. (**A**) Schematic illustration of a single 9.1 kb repeat of the rDNA in *S. cerevisiae* found on Chr. XII. Position of the RFB, origin of DNA replication (*ARS*), *35S* rRNA (*35S*) and *5S* rRNA (*5S*) genes are indicated. Position of probe used for Southern blotting and *Bgl*II cleavage sites used for the 2D DNA gel are also shown. The RFB allows progression of the replication fork in the same direction as 35S rRNA transcription, but not in the opposite direction when Fob1p is bound to the sequence (**B**) Fob1p expression after different times of galactose induction (0, 60, 120, 240 and 360 min) together with negative controls (non-inducing conditions) on strain LBy-365. (**C**, upper panel) Outline of yeast culture treatment preceding isolation of DNA for 2D DNA gel analyses. (C, lower panel) 2D DNA gel analysis (strain LBy-413)

(continued)

The *GAL1,10* inducible promoter enables us to obtain a rapid induction of *FOB1*, when cells are grown in the presence of galactose (Figure 1B). To further verify that the Fob-block system has active RFBs on *FOB1* induction, we performed classical neutral/neutral 2D gel analyses for the rDNA locus. We analysed a DNA fragment that would run as a simple Y-structure. If replication fork arrest occurs at the RFBs, partially replicated molecules will accumulate and give a distinctive dot on the Y-arc. Cells were grown as outlined in Figure 1C (top). As control, a yeast culture was also grown under repressed conditions. A dot is seen on the Y-arc at 40 and 60 min after release from the G1 block under inducing conditions (Figure 1C, bottom), but not during repressed conditions. Furthermore, a comparison of the *GAL-FOB1* and a wild-type strain, where *FOB1* is expressed from its endogenous promoter, reveals a significant higher level of fork stalling at the RFB site in *GAL-FOB1* cells relative to wild-type cells, as visualized by the appearance of the distinctive dot in 2D gels (Figure 1D).

In conclusion, the Fob-block system allows induction of active protein–DNA barriers in the rDNA, which lead to replication fork stalling.

Growth of Fob-block cells requires the MRX complex, but not homologous recombination

Wild-type Fob-block cells were next tested by comparing growth of cells on glucose (*FOB1* OFF) with growth on galactose (*FOB1* ON). The *GAL-FOB1* strain does not show any significant growth defect on galactose compared with a wild-type strain, demonstrating that cells with the Fob-block system are able to efficiently overcome induced RFBs without significantly affecting cell growth (Figure 2A).

In *S. cerevisiae*, forks arrested at RFBs in the rDNA may be prone to collapse and thereby recombine (27). Indeed, replication- and *FOB1*-dependent DNA breaks have been mapped to the RFB regions (28). On the contrary, when RFBs are taken out of the rDNA context, fork arrest does not give rise to observable recombination, and survival does not depend on Rad52 (14). To investigate whether our Fob-block system requires HR for cell survival, the *GAL-FOB1* strain was combined with deletions of central components of the *RAD52* epistasis group, and cell growth was tested. Deletion of either *RAD52* or *RAD51* in the *GAL-FOB1* strain did not give rise to any growth defects on galactose plates relative to a *RAD52* or *RAD51* deletion mutant without the Fob-block system (Figure 2B). This reveals that recovery from the induced RFBs is independent of HR.

Surprisingly, when the different components of the MRX complex were deleted (*MRE11*, *RAD50* or *XRS2*) in the *GAL-FOB1* strain, a strong growth defect was observed on galactose plates for all strains relative to the *MRE11*, *RAD50* or *XRS2* deletion mutants alone (Figure 2C). This highlights a need for MRX to cope with active RFBs, although HR *per se* is not required. Interestingly, even though active RFBs are a normal feature of rDNA, overexpression of Fob1 adds a pressure on the cell, which allows for identification of

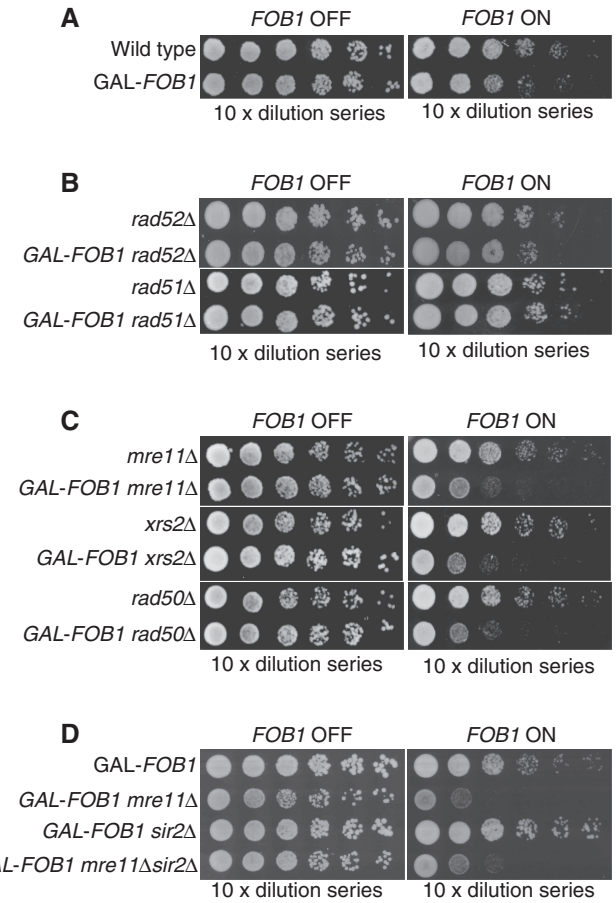

Figure 2. Fob-block cells require the MRX complex, but not homologous recombination for proper cell growth. Also, 10-fold serial dilutions of raffinose-grown cultures (non-induced) were spotted on glucose and galactose plates. (**A**) Shown are isogenic strains of wild-type (LBy-1), *GAL-FOB1* (LBy-413) (**B**) Shown are isogenic strains of *rad52*Δ (LBy-108), *GAL-FOB1 rad52*Δ (LBy-588), *rad51*Δ (LBy-14), *GAL-FOB1 rad51*Δ (LBy-612) (**C**) Shown are isogenic strains of *mre11*Δ (LBy-605), *GAL-FOB1 mre11*Δ (LBy-756), *xrs2*Δ (LBy-80), *GAL-FOB1 xrs2*Δ (LBy-774), *rad50*Δ (LBy-615), *GAL-FOB1 rad50*Δ (LBy-581). (**D**) *sir2*Δ does not suppress the *mre11*Δ growth defect. Shown are isogenic strains of *GAL-FOB1* (LBy-413), *GAL-FOB1 mre11*Δ (LBy-756), *GAL-FOB1 sir2*Δ (LBy-888), *GAL-FOB1 mre11*Δ *sir2*Δ (LBy-909).

Figure 1. Continued
reveals replication fork stalling in the rDNA (Chr. XII) during inducing conditions (*FOB1* ON), but not during non-inducing conditions (*FOB1* OFF); see text for details. (**D**) 2D DNA gel analyses conducted to compare replication fork stalling efficiency at the RFB between a wild-type (LBy-1) strain with endogenous levels of Fob1 and a strain (LBy-413) with overexpression of Fob1. During the experiment, the wild-type strain was kept in glucose medium to give optimal conditions for this strain, whereas LBy-413 was treated as indicated above the 2D gel. Both strains were synchronized. On the right is shown a quantification of replication fork stalling (see 'Material and Methods' section for further explanation), and in the middel is shown FACS profiles for the strains. The *n* and 2*n* is DNA content in G1 and G2, respectively.

proteins required for cells to cope with RFBs or for normal fork integrity of the unblocked forks.

Binding of the Fob1 protein to RFB not only promotes polar replication fork arrest but also loads the NAD-dependent histone deacetylase Sir2 at the RFB via a protein complex called regulator of nucleolar silencing and telophase exit (29,30). Loading of Sir2 is known to cause rDNA silencing, which suppresses intrachromatid recombination. To establish whether requirement for the MRX complex on overexpression of Fob1 is due to replication fork stalling or Sir2 mediated at the rDNA, we performed growth analysis of a *GAL-FOB1 sir2*Δ deletion strain and a *GAL-FOB1 mre11*Δ*sir2*Δ strain. Absence of *SIR2* does not give rise to any growth defect in our *GAL-FOB1* strain, and the growth defect scored in the absence of *MRE11* is not suppressed by a *SIR2* deletion (Figure 2D). This supports the idea that the MRX complex is required at the rDNA owing to replication fork stalling and not owing to an affected rDNA silencing on overexpression of Fob1.

In conclusion, our genetic data unravel a recombination independent function of MRX for cell growth on increased replication fork stalling in the rDNA locus.

Absence of the MRX complex leads to more ssDNA at protein–DNA barriers

As the Fob-block system is insensitive to the lack of Rad51 and Rad52, overexpression of Fob1 neither seems to induce more DSBs *per se*, which require HR for repair, nor to generate a need for HR-dependent fork restart at RFBs. It is thus unlikely that the need for MRX at active RFBs derives from its well-established role in early resection upstream of HR (31–33) or its scaffold role for recruiting the more extensive resection machinery (34,35).

To further support this rationale, we investigated the behaviour of a well-characterized Mre11 mutant, which is endo- and exonuclease deficient (*mre11*-H125N), in our Fob-block system. Spot assays reveal that these enzymatic activities of Mre11 are not required for growth during conditions, where RFBs are induced (Figure 3A). We therefore rule out a function of the MRX complex in early resection. Next, an *mre11*Δ *yku70*Δ double mutant was generated in our *GAL-FOB1* strain to test whether deletion of *YKU70* would suppress the growth defect of an *MRE11* deletion. It has previously been shown that the *mre11*Δ IR sensitivity is suppressed by *YKU70* deletion. This is thought to originate from the loss of end protection by Ku, which then would allow DSB ends to be processed even in the absence of Mre11 (36,37). When the *GAL-FOB1 mre11Δ yku70Δ* strain was analysed, a growth defect comparable with that of the *mre11*Δ single mutant was observed (Figure 3B). All together, this supports the notion that MRX accomplishes a task at RFBs, which is not directly connected with its role in DSB processing.

To establish whether the structural features intrinsic to the MRX complex is needed to cope with protein–DNA barriers, we took advantage of the $rad50^{sc}$ and $rad50^{sc+h}$ mutants. The $rad50^{sc}$ mutant is altered in the CXXC domain compromising hook–hook interactions, whereas the $rad50^{sc+h}$ mutant carries a truncated coiled-coil domain, which shortens the length of the molecular tether by 243 aa. Despite these structural alterations, the MRX complex remains intact in $rad50^{sc}$ and $rad50^{sc+h}$ mutants, and homologous recombination functions are largely unaffected in the $rad50^{sc+h}$ mutant (38). We coupled the two mutants with our Fob-block system and investigated growth by spot assays. The *GAL-FOB1* $rad50^{sc}$ strain displays the same growth defect as a *GAL-FOB1 mre11Δ* strain on galactose, whereas the *GAL-FOB1* $rad50^{sc+h}$ strain shows a milder but reproducible growth defect compared with the *GAL-FOB1 mre11* strain (Figure 3C). Together, these data underscore the importance of the hook and coiled-coil domains of Rad50 for proper growth when protein–DNA barriers are induced, and thereby strongly points to molecular bridging being required at protein–DNA barriers.

We thus seek a function for the MRX complex, which is DSB independent, but pivotal for the cell on increased replication fork stalling in the rDNA. One such function could be as a fork stabilizer as has previously been suggested for HU-stalled forks (39). If replication forks stalled at protein–DNA barriers are unstable in the absence of a competent MRX complex, this may lead to more DSBs in the rDNA. We thus tested whether more DSBs could be scored in the rDNA in the *GAL-FOB1 mre11*Δ strain using a DSB assay previously described (28,40). Although the majority of DSBs found for wild-type cells at the rDNA has been suggested to be a result of pre-existing nicks, which are insensitive to normal DSB repair processing (41), elevated levels of DSBs have been demonstrated in different mutants (40–42). Figure 3C shows an autoradiogram obtained with a probe recognizing a sequence located between *5S* and the RFB. Consistent with previous reports, we obtain two bands in all samples, migrating below the digested rDNA units (M) and representing S-phase independent DSBs (28). Furthermore, we also detect the S-phase specific DSB at 40 min (28). Importantly, no obvious difference in the level of the DSBs are detected between *GAL-FOB1* and *GAL-FOB1 mre11Δ* cells, which suggests that absence of Mre11 does not give rise to a significant elevated level of DSBs around the RFB site in the rDNA. Even suppressing DSB repair by a *RAD52* deletion (*GAL-FOB1 mre11Δ rad52Δ*) does not enable us to detect more DSBs in the rDNA (Figure 3C).

From our DSB assay, we notice an accumulation of DNA structures in the absence of Mre11, which fail to migrate into the gel at the later time points. Although replication dependent, these structures do not represent unreplicated DNA, as they are not detected during early DNA replication (40-min sample) in *GAL-FOB1* and *GAL-FOB1 mre11Δ* cells, but accumulate after bulk DNA synthesis has taken place according to FACS analyses. Furthermore, the DNA structures are formed in a recombination independent way, as retention is also observed in *GAL-FOB1 mre11Δ rad52Δ* cells.

To further investigate this phenomenon, we analysed genomic DNA using the well-established pulsed field gel electrophoresis (PFGE) method. In PFGs, linear DNA migrates according to its size, whereas branched structures

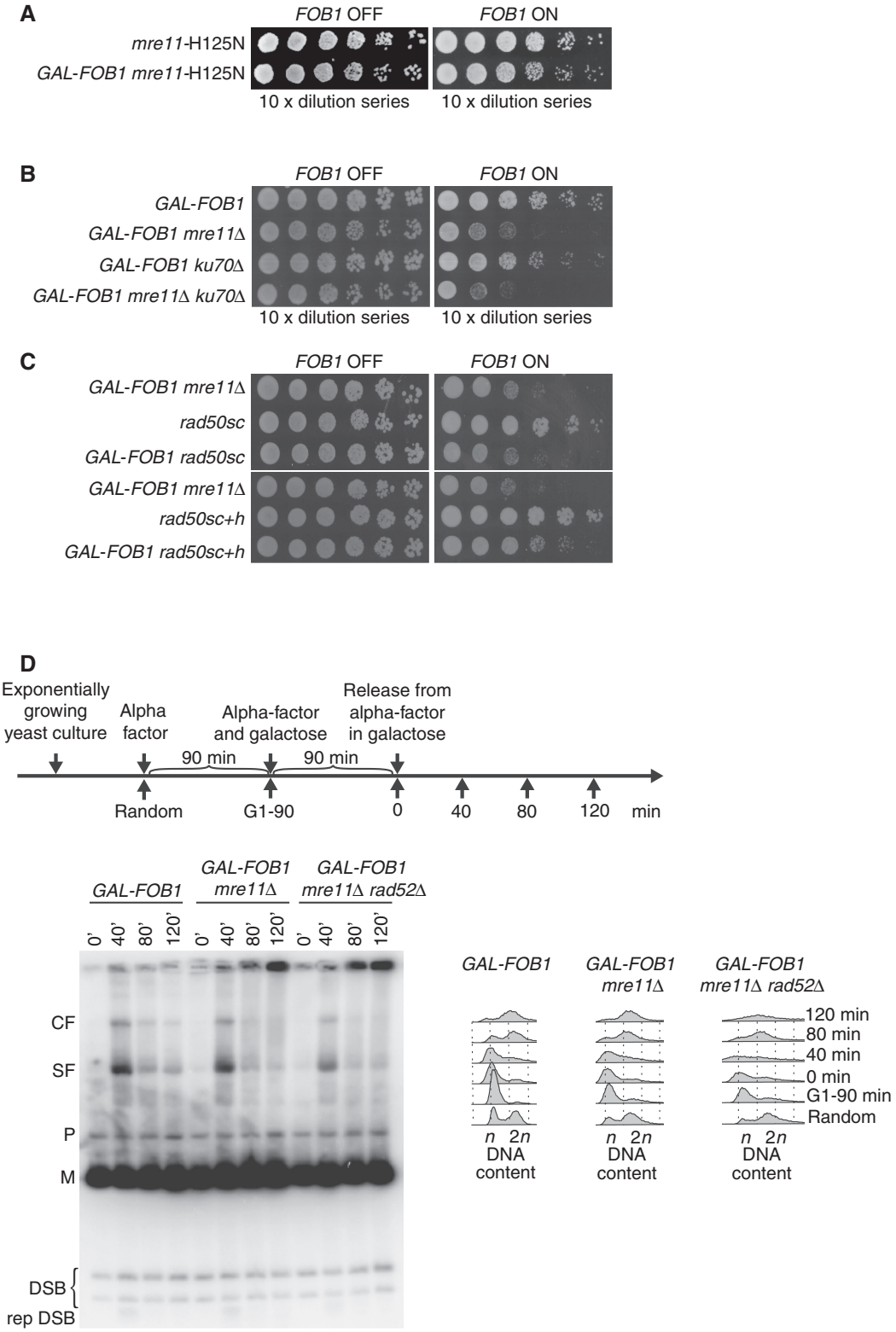

Figure 3. The MRX complex plays a DSB independent role at RFBs (**A**) Shown are isogenic strains of *mre11*-H125N (LBy-623), *GAL-FOB1 mre11*-H125N (LBy-631). (**B**) Deletion of *KU70* does not suppress the phenotype of *GAL-FOB1 mre11* mutant. Shown are isogenic strains of *GAL-FOB1* (LBy-413), *GAL-FOB1 mre11*Δ (LBy-756), *GAL-FOB1 ku70*Δ (LBy-905) and *GAL-FOB1 mre11*Δ *ku70*Δ (LBy-903). (**C**) Molecular bridging is required by MRX complexes is required at protein–DNA barriers. Shown are isogenic strains of *GAL-FOB1 mre11*Δ (LBy-756), $rad50^{sc}$ (LBy-1061), *GAL-FOB1* $rad50^{sc}$ (LBy-1070), $rad50^{sc\ +\ h}$ (LBy-1062) and *GAL-FOB1* $rad50^{sc\ +\ h}$ (LBy-1071) (**D**) Absence of Mre11 does not generate more DSBs in the rDNA, but abnormal structures are detected. Shown is a DSB assay for *GAL-FOB1* (LBy-413), *GAL-FOB1 mre11*Δ (LBy-756) and *GAL-FOB*1 *mre11*Δ *rad52*Δ (LBy-680). Digested rDNA units (M), partial digested rDNA units (P), converging forks (CF), stalled forks at RFB (SF), replication independent DSBs (DSB), replication dependent DSB (rep DSB).

as well as replication and recombination intermediates do not enter the gel and remain trapped in the wells. Cells were processed as schematically shown in Figure 4A, and DNA isolated in agarose plugs was analysed by PFGE. Figure 4B shows an EtBr stain of the PFG as well as a Southern blot obtained with probes recognizing Chr. XII and Chr. II. From this, it is evident that Chr. XII fails to fully enter the gel after bulk DNA synthesis has occurred in the absence of *MRE11* (as evident from FACS analysis presented in Figure 4C). Quantification of the Southern

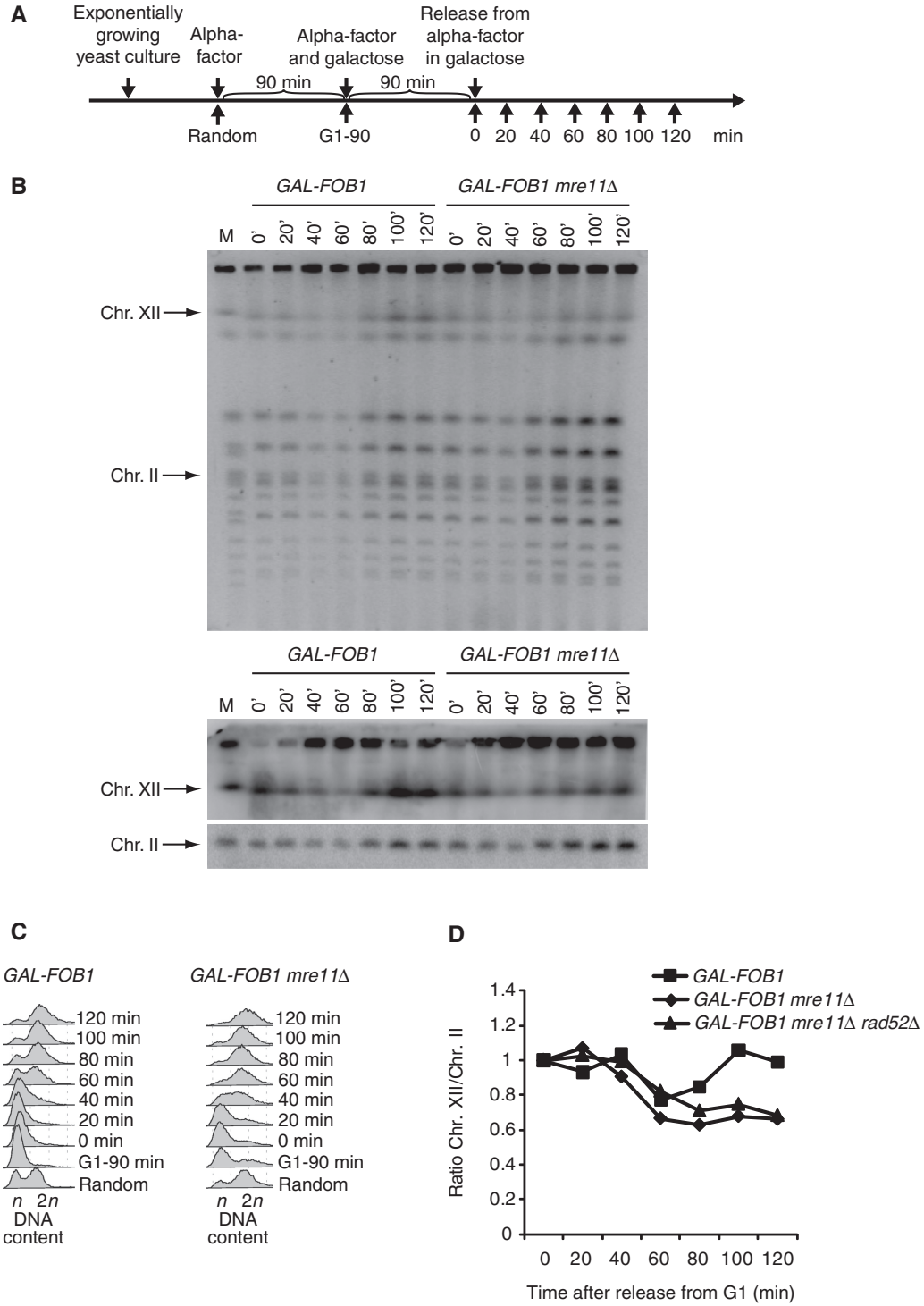

Figure 4. Chr. XII partly fails to migrate into the gel in a Fob-block *mre11Δ* strain. (**A**) Outline of yeast culture treatment before PFGE analysis. (**B**) Shown are PFGE analysis for *GAL-FOB1* (LBy-413) and *GAL-FOB1 mre11*Δ (LBy-756) cells. The upper panel shows ethidium bromide staining of gel, and the lower panel shows Southern blotting of the same gel with probes recognizing Chr. XII and Chr. II, respectively. (**C**) FACS analysis on samples taken for PFGE analysis. (**D**) Quantification of the amount of Chr. XII entering the gel relative to Chr. II. Included is also quantification done for the *GAL-FOB1 mre11Δrad52*Δ strain (LBy-680). See 'Material and Methods' section for further details.

blot reveals that ~40% of Chr. XII remains in the wells in the absence of *MRE11* (Figure 4D). This suggests that either branched structures, replication intermediates or recombination intermediates are frequently formed in *GAL-FOB1 mre11Δ*. As *GAL-FOB1 mre11Δ rad52Δ* cells still retain DNA in the wells, we can conclude that the retained structure is not a true recombination intermediate (only quantification is shown for *GAL-FOB1 mre11Δ rad52Δ* in Figure 4D).

To investigate whether the retained structure contains any ssDNA, we performed ChIP using anti-Rfa1 antibody. Extensive levels of ssDNA may inhibit proper restriction digestion in our DSB assay, which could explain why DNA is retained in the wells in this assay. ChIP experiments were performed with the *GAL-FOB1* and the *GAL-FOB1 mre11Δ* strains, where the experimental setup was as schematically shown in Figure 3C. Recovered DNA was analysed using three primer sets located in close proximity to the RFB sequence in the rDNA (Figure 5A). During S–phase, there is a slight increase in recovered RPA for both strains (Figure 5B, 40-min timepoint). Oppose to the *GAL-FOB1* strain, where recovered RPA decreases at the late time points of the experiments absence of Mre11 leads to an accumulation of RPA in late S-G2 phase. Thus, we recover a 2–3-fold increase of RPA in proximity to the RFB 80 and 120 min after release of cells into the S phase (Figure 5B). As we do not recover RPA above background at Chr. III in *GAL-FOB1 mre11Δ*, our data suggest that the structures accumulating in the rDNA in the absence of Mre11 includes RPA coated ssDNA. Increased levels of ssDNA in the rDNA are not intrinsic to lack of Mre11, as an *mre11Δ* strain does not give rise to more ssDNA compared with the *GAL-FOB1* strain relative to the *GAL-FOB1* strain (Supplementary Figure S1).

In summary, we discover an endo- and exonuclease independent role for the MRX complex for DNA integrity at RFBs, where absence of MRX leads to an accumulation of DNA structures at the rDNA after bulk DNA synthesis, which are retained in the wells in a PFG. Furthermore, lack of MRX results in a higher level of RPA binding in the rDNA, which suggests that the retained DNA structure contains regions of ssDNA.

Ectopically placed RFBs but not RFBs in the rDNA trigger a checkpoint response in the absence of MRX

To test whether the higher levels of ssDNA observed in the absence of the MRX complex activate a checkpoint response, Rad53 activation was investigated using the *in situ* autophosphorylation assay (ISA) (26).

Rad53 activation was first investigated in the *GAL-FOB1* strain. Cells were grown as shown schematically in Figure 6A. In accordance with our spot assays, where normal growth on galactose is observed, we do not detect any Rad53 activation in this strain (Figure 6B). Next, *GAL-FOB1 mre11Δ* was tested. To our surprise, we failed to detect Rad53 activation in the *GAL-FOB1 mre11Δ* strain (Figure 6C), which could indicate that either the amount of ssDNA accumulating in the absence of Mre11 is not sufficient to trigger a checkpoint response or alternatively, checkpoint activation is suppressed in this chromosomal context.

To differentiate between these options, we set out to investigate whether a checkpoint can be provoked if RFBs are inserted in another chromosomal context. We contructed a strain with a triplicate of RFB sequences inserted ectopically in a non-transcribed region on chromosome VI between the early firing origins *ARS606* and *ARS607* (*GAL-FOB1* eRFB where e denotes ectopically). We chose this chromosomal locus, as we have previously used this to study responses to a single protein–DNA adduct (21). The rationale behind insertion of RFB triplicates and not only a single RFB sequence at this locus was to increase the percentage of cells in a culture with active RFBs (we still only expect binding of one Fob1 owing to constrain). Checkpoint activation was next investigated in two strains, *GAL-FOB1* eRFB and *GAL-FOB1* eRFB *mre11Δ*. As expected, the *GAL-FOB1* eRFB did not give rise to checkpoint activation (Figure 6E), whereas we obtain robust Rad53 activation, when Mre11 is absent. Checkpoint activation is detectable in the *GAL-FOB1* eRFB *mre11Δ* strain at 90 min after release from the G1 arrest, giving more robust signals 105 min after release, which coincides with the late S/G2 phase of the cell cycle as revealed from FACS analysis (Figure 6E). Although the *GAL-FOB1* eRFB *mre11Δ* strain has activated checkpoint, this does not influence cell growth, as the scored growth defect for this strain is comparable with that observed for the *GAL-FOB1 mre11Δ* strain (Figure 6F).

Although we do not expect that several Fob proteins are able to bind at these triplicates owing to constrain in the amount of base pairs available for wrapping around the Fob1 protein, we confirmed that the checkpoint activation observed for the *GAL-FOB1* eRFB *mre11Δ* was not due to increased 'strength' of the ectopic protein–DNA barrier relative to those in the rDNA compartment. Thus, checkpoint activation was investigated in a strain where only one RFB sequence was inserted between *ARS606* and *ARS607*. As evident from Supplementary Figure S2, absence of *MRE11* in this strain leads to a robust checkpoint activation much alike what was observed for the *GAL-FOB1* eRFB *mre11Δ* strain (Figure 6E). Thus, checkpoint activation in the *GAL-FOB1* eRFB *mre11Δ* strain cannot be explained by a difference in RFB strength. Furthermore, to rule out that homologous recombination is required at ectopic RFBs owing to different processing compared with RFBs in the rDNA, and thus could explain the difference in checkpoint activation, we generated a *GAL-FOB1* eRFB *rad52Δ* mutant and investigated growth. These spot assays confirm that Rad52 is not required for cells to overcome an ectopic protein–DNA barrier, and thus in this respect, there is no difference between ectopic RFBs and RFBs in the rDNA (Supplementary Figure S3).

Taken together, the results demonstrate that absence of MRX leads to robust checkpoint activation when ectopically placed RFBs are present; on the contrary, although RPA-containing DNA is present at the rDNA, this fails to induce a detectable checkpoint response.

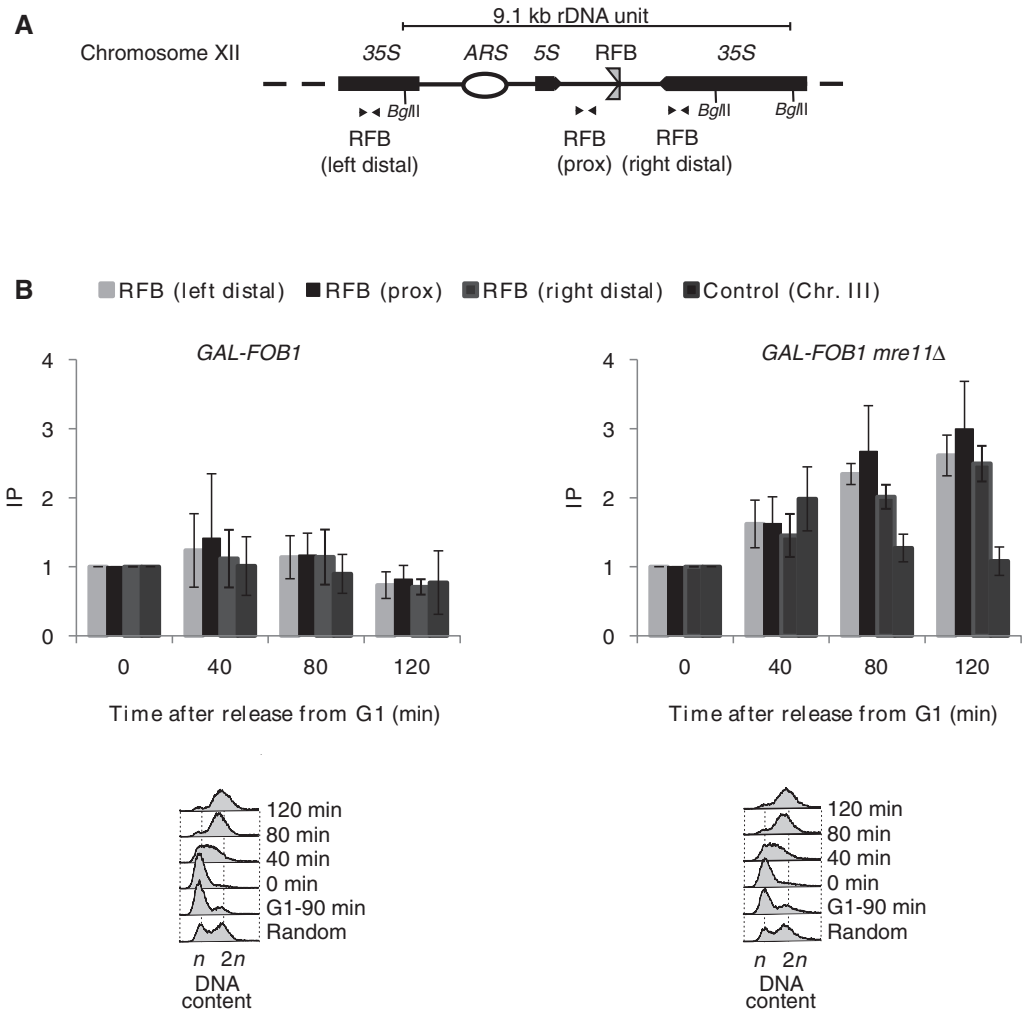

Figure 5. RPA accumulates on replication fork stalling at the RFB in the rDNA. (**A**) Schematic illustration of a single rDNA unit with the positions of the primers used for real-time PCR shown (**B**) ChIP was performed using antibody against RPA (Rfa1) on synchronized cells from *GAL-FOB1* (LBy-413) and *GAL-FOB1 mre11Δ* (LBy-756) strains. Time (min) after release from alpha-factor block is indicated below each graph. Regions in near proximity to the RFB site [(RFB (prox)] and distal to the RFB site [RFB (right distal) and RFB (left distal)] were amplified by real-time PCR. Enrichment of RPA around the RFB site was plotted as fold increase of immunoprecipitated DNA over beads alone. Fold increase of time point 0 sample was set at 1. Error bars, s.d. ($n = 3$). A representative FACS profile for *GAL-FOB1* (*LBy-475*) and *GAL-FOB1 mre11*Δ (*LBy-545*) are shown (lower panel). *n* and *2n* are DNA content in G1 and G2, respectively.

From the previous analysis, we do not know whether the *ARS606–ARS607* region is fully replicated. If the MRX complex is a general replication fork stabilizer, the rightward-moving fork (coming from *ARS606*) may encounter problems in the absence of the MRX complex. Thus, we cannot rule out that the observed checkpoint activation is merely due to problems in the *ARS606–ARS607* region rather than problems arising directly at the ectopically placed RFB in the absence of the MRX complex. To investigate the fate of the rightward-moving fork, we entertained the idea that if this fork encounters problems, it would lead to either delayed replication or unreplicated DNA in the *ARS606–ARS607* region.

Fluorescence microscopy was used to study the potential presence of unreplicated DNA in near proximity to the RFBs at Chr. VI. A TetO array was inserted in the *ARS606–ARS607* region close to the RFBs in *GAL-FOB1* eRFB and *GAL-FOB1* eRFB *mre11Δ* strains (Figure 7A). We anticipated that a single Tet repressor (TetR)-RFP focus would exist in the G1 phase of the cell cycle, whereas two foci would be present in late S/G2 phase of the cell cycle in the case of normal replication of the region. To be able to score two dots independently of the segregation event, we combined our *GAL-FOB1* eRFB TetR-TetO and *GAL-FOB1* eRFB TetR-TetO *mre11Δ* strains with a ts allele of *SCC1* (*scc1-73*), which at 34°C will result in sister chromatid cohesion failure (43). This will allow us to detect two dots before actual segregation due to 'breathing' of the sister chromatids. Cells were synchronized in G1, and Fob1 induced to activate the RFB, whereas Scc1 was inactivated at 34°C, before cells were released into S-phase at 34°C to keep Scc1 inactivated. At the indicated times, cells were analysed by fluorescence microscopy to score the presence of one or two (TetR)-RFP dots (Figure 7B).

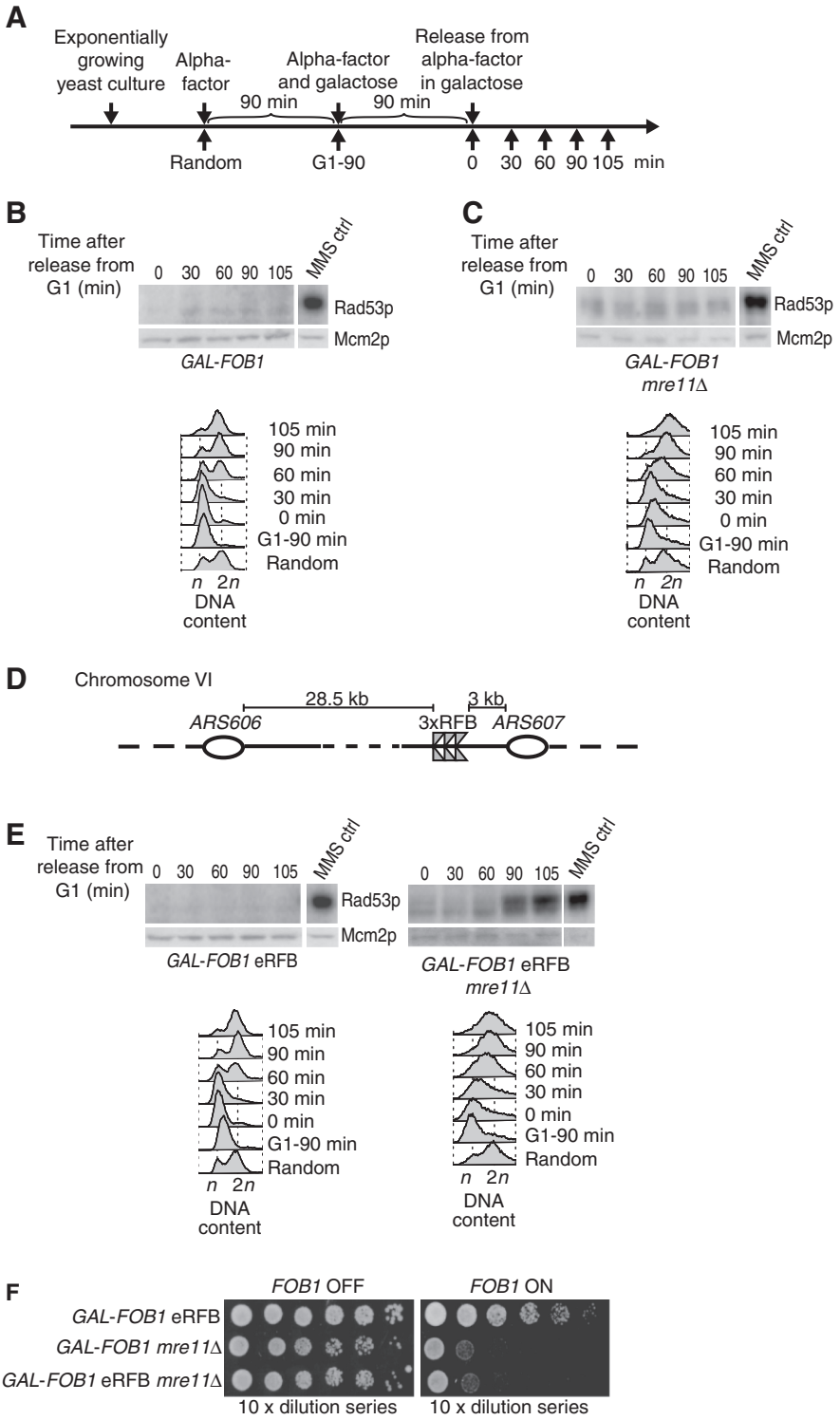

Figure 6. Ectopically placed RFBs but not RFBs in the rDNA trigger a checkpoint response in the absence of Mre11. (**A**) Outline of yeast culture treatment preceding ISA. (**B**) The *GAL-FOB1* (LBy-413) strain does not trigger checkpoint activation on induction of protein–DNA barriers. (**C**) A checkpoint response is not activated, despite growth problems and RPA accumulation in the *GAL-FOB1 mre11*Δ strain (LBy-756). (**D**) Schematic representation of the modified Fob-block system at Chr. VI with ectopic RFBs inserted close to *ARS607*. (**E**) Absence of *MRE11* leads to checkpoint activation when active protein–DNA barriers are present ectopically on Chr. VI in the *GAL-FOB1* eRFB *mre11*Δ strain (LBy-649). Checkpoint activation was also investigted for a *GAL-FOB1* eRFB strain (LBy-439). For all kinase assays shown, equal amount of yeast extract was loaded on 10% SDS–polyacrylamide gels. For each strain, the upper box shows the incorporation of [γ-^{32}P] adenosine triphosphate into Rad53p and the bottom panel a western for Mcm2p on the same blot. Time (min) after release from alpha-factor block is indicated above each gel. MMS control (ctrl) is 5 µl of a sample containing a fixed amount of MMS-activated Rad53p standard, which is used for internal control of the kinase assays and allows comparison between gels. Samples shown together and with the same MMS ctrl have been loaded on the same gel. FACS samples were taken throughout the experiments and cell cycle profile displayed below each gel. (**F**) Spot assays performed as in Figure 2 for the isogenic strains *GAL-FOB1* eRFB (LBy-439), *GAL-FOB1 mre11*Δ (LBy-756), *GAL-FOB1* eRFB *mre11*Δ (LBy-649).

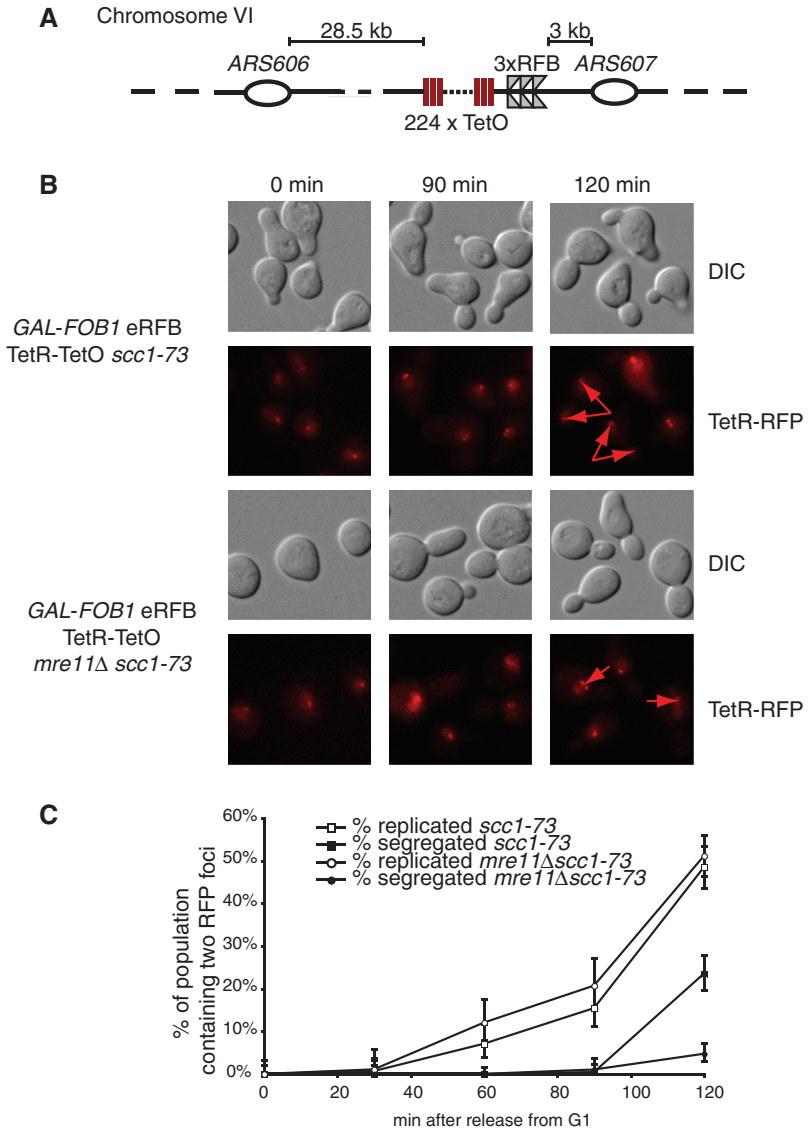

Figure 7. Checkpoint activation is a direct cause of the ectopically placed RFB (**A**) Schematic representation of the modified Fob-block system with a TetO-array. (**B**) The *ARS606–ARS607* region is fully replicated as measured by fluorescence microscopy on strain *GAL-FOB1* eRFB TetR-TetO *scc1-73* (LBy-868) and *GAL-FOB1* eRFB TetR-TetO *mre11Δ scc1-73* (LBy-880). Fluorescence (TetR-RFP) and differential interference contrast images (DIC) of representive cells. Arrowheads mark foci. (**C**) Quantification of cells containing two RFB foci and of cells with segregated foci. At each time point, 100–300 cells were examined for RFB foci.

Two dots are seen in the *GAL-FOB1* eRFB *mre11Δ* strain, revealing that replication takes place in the *ARS606–ARS607* region. As shown graphically, there is no difference in the timing of appearance of two dots in the two strains, and the percentage of cells with the locus replicated is also the same (Figure 7C). However, absence of *MRE11* leads to a significant delay in the segregation process, which may be explained by the basal level of checkpoint activation, which we always detect for *mre11Δ* cells. Alternatively, the accumulation of late replication intermediates or branched structures we observed in the absence of MRE11 in our Fob-block system could also account for this delayed segregation.

As we fail to detect unreplicated DNA in the *ARS606–ARS607* region, we conclude that the rightward-moving fork is replication competent throughout this region. Thus, neither problems for the active fork nor unreplicated DNA is the checkpoint-causing event. Instead our data strongly suggest that it is an incidence directly at the ectopic RFBs, which generates the checkpoint-activating structure in the absence of the MRX complex. Thus, problems at a protein–DNA barrier at its natural cellular chromosomal context do not generate a detectable checkpoint signal, whereas placed ectopically, it causes a robust checkpoint-activating signal.

Chromatin context dictates checkpoint activation

The aforementioned data suggest that chromosomal context may have an influence on checkpoint signalling. Induction of the Fob-block system will likely affect the level of rDNA silencing, as more Sir2 will be recruited to the RFBs via the regulator of nucleolar silencing and

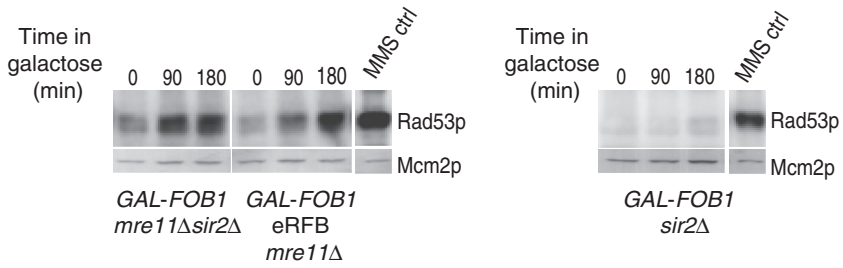

Figure 8. Sir2 suppresses the checkpoint response in the rDNA. ISA was performed on asynchronous yeast cultures of *GAL-FOB1* eRFB *mre11*Δ (LBy-649), *GAL-FOB1 mre11*Δ *sir2*Δ (LBy-909) and GAL-FOB1 sir2Δ (LBy-888) strains. Samples were taken before galactose induction and after 90 and 180 min of induction. The kinase assay was performed as described in 'Material and Methods' section and in Figure 6.

telophase exit complex (29,30). Although we find that a *SIR2* deletion does not rescue the slow growth phenotype of an *MRE11* deletion in our Fob-block system, we cannot rule out that a higher level of rDNA silencing may affect the checkpoint response. To examine this, we investigated Rad53 activation in a *GAL-FOB1 mre11Δ sir2Δ* strain. This experiment was conducted with asynchronous yeast cultures, as *sir2Δ* strains are insensitive to alpha factor treatment. Samples were taken before galactose induction and after 90 and 180 min of induction. As a positive control for this experiment, we included the *GAL-FOB1* eRFB *mre11Δ* strain, and checkpoint activation was also investigated in a *GAL-FOB1 sir2Δ* strain. Excitingly, Rad53p activation now occurs in the *GAL-FOB1 mre11Δ sir2Δ* strain to approximately the same level as seen for the *GAL-FOB1* eRFB *mre11Δ* strain, whereas deletion of *sir2Δ* alone in the *GAL-FOB1* strain does not give rise to checkpoint activation (Figure 8). We cannot rule out that more DSBs are generated in the *GAL-FOB1 mre11Δ sir2Δ* cells, and that this is the checkpoint-causing event. Indeed, a triple mutant *GAL-FOB1 mre11Δ sir2Δ rad52Δ* is extremely slow growing compared with any of the double mutant combinations, which demonstrates a requirement for homologous recombination when both Mre11 and Sir2 are absent (data not shown). This slow growth is, however, totally independent on *FOB1* induction opposed to the observed checkpoint activation, which requires *FOB1* induction. Thus, checkpoint activation is caused by events, which are triggered by a protein–DNA barrier.

In summary, our results demonstrate that by alleviating Sir2-mediated rDNA silencing, cells are now able to provoke a checkpoint response from within the rDNA when the MRX complex is absent. The results suggest that rDNA silencing not only controls recombination but also suppresses proper checkpoint response at least in the vicinity of the RFB.

DISCUSSION

Our study reveals several novel observations. First, we uncover a DSB-independent function of the MRX complex for DNA integrity at protein–DNA barriers in the rDNA, where absence of the MRX complex leads to increased levels of ssDNA. Second, we find that absence of Mre11 does not trigger a checkpoint response from within the rDNA, whereas its absence leads to checkpoint activation when ectopically placed RFBs are present. Third, relieving rDNA silencing is sufficient to provoke checkpoint activation in the rDNA to the same extent as seen for the ectopic site, strongly suggesting that checkpoint activation is governed by chromatin context at least in the rDNA.

In our Fob-block system, all events caused by higher levels of stalled replication forks in the rDNA are unproblematic for wild-type cells but become detrimental when cells lack MRX. This is in agreement with genetic data reporting that absence of Rrm3, a helicase required for helping replication forks traverse protein–DNA barriers, leads to synthetic lethality with *mre11Δ*, *rad50Δ* and *xrs2Δ* (44). Although overexpression of Fob1 likely affects the level of rDNA, silencing deletion of *SIR2* does not suppress the growth defect observed in the absence of the MRX complex. This supports the idea that the MRX complex is required at the rDNA owing to replication fork stalling and not owing to an affected rDNA silencing on overexpression of Fob1.

We provide evidence for a DSB independent role of MRX at protein–DNA barriers based on three facts. First, *RAD52* is not required for proper cell growth in our Fob-block system, which argues against DSB formation. Second, the growth defect observed for *GAL-FOB1 mre11Δ* cells is not suppressed by a *YKU70* deletion. It has previously been reported that suppression of *mre11Δ* phenotypes by a *YKU70* deletion is restricted to events at DSB ends (37). Third, the endo- and exonuclease activities of Mre11p are not required.

At present, we do not know the exact mechanism by which MRX protects forks at RFBs; however, several modes of action can be envisioned, which are not mutually exclusive. MRX may preserve the conformation of newly synthesized DNA behind forks at RFBs, thus preventing replisome collapse. This function would be analogous to what has been suggested for MRX at HU-stalled forks and is supported by structural data showing that the MRX complex can bridge two DNA duplexes held in the same distance as newly synthesized sister chromatids (39,45). Alternatively, the MRX complex may prevent fork reversal at RFBs (Figure 9A). At so-called terminal forks, absence of the Mre11 has been suggested to lead to fork reversal, where the generated structure is prone to cleavage (46). If fork reversal occurs at RFBs in the absence of Mre11, it does not

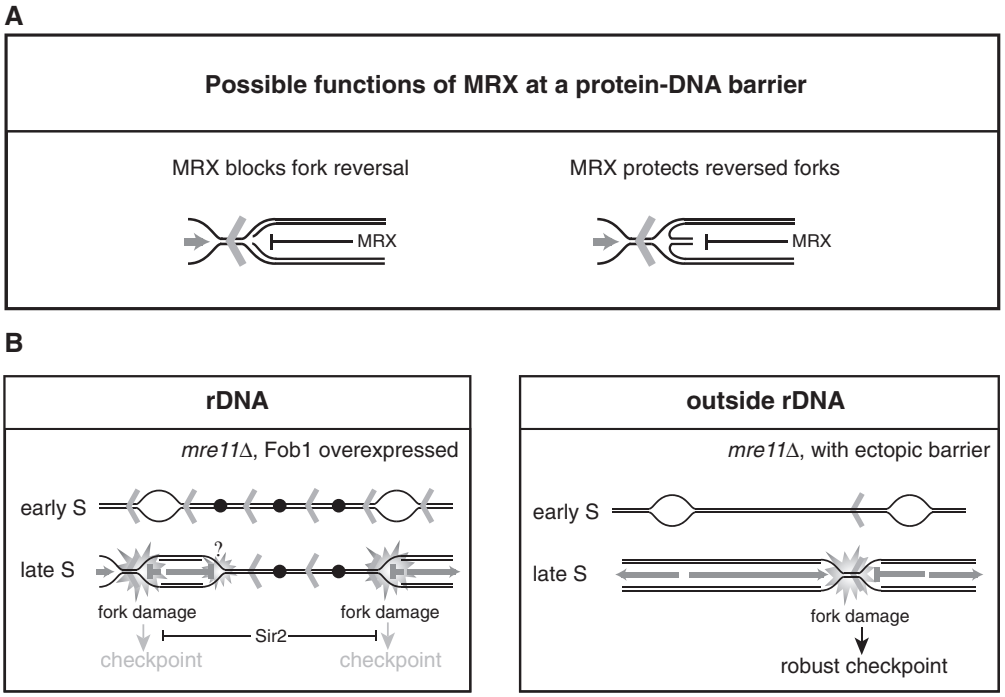

Figure 9. (**A**) Suggested functions of the MRX complex on replication fork stalling at a protein–DNA barrier. The MRX complex may hinder fork reversal (left) or protect a reversed fork from further processing (right). (**B**) Model for the cellular consequences to elevated levels of replication fork stalling in the rDNA (left panel), and for ectopically placed RFBs (right panel) in *mre11*Δ cells. Fob1 induction generates a higher level of active RFBs in the rDNA, which have detrimental effect on growth when the MRX complex is absent. The growth defect may stem from problems arising directly at the RFBs; however, as replication in the rDNA is challenged by its repetitive nature where unusual structures have the potential to form, fork stalling at other places than the RFB may be a frequent event. Together, this creates a strong need for the MRX complex either to suppress fork reversal or protect reversed forks in the rDNA. When the RFB sequence is placed ectopically, the MRX complex is required at the protein–DNA barrier as the rightward-moving fork is replication competent throughout the *ARS606–ARS607* region. Aberrant structures generated in the absence of the MRX complex are checkpoint blind in the rDNA owing to the presence of Sir2, whereas ectopically placed RFBs provoke a checkpoint signal in the absence of the MRX complex. Open bubbles represent active origins, whereas black dots represent inactive origins. Red arrowheads represent Fob1-bound RFB sequences.

seem to be prone to cleavage, as we fail to detect higher levels of DSBs at the RFBs in the rDNA. However, our PFGE analysis supports the idea that absence of the MRX complex could lead to more branched structures in the rDNA, as a large portion of Chr. XII is retained in the wells. The retention of DNA in the wells in the DSB assays more likely stems from an inhibition of restriction enzyme digestion owing to the presence of ssDNA, as branched structures will run into this type of gel. Furthermore, we detect more RPA in the rDNA at late time points (after bulk DNA synthesis) in the absence of Mre11. This indicates that processing occurs in these cells generating more ssDNA compared with wild-type cells. This can be explained if more reversed forks are generated in the absence of MRX, which are processed to give ssDNA. Indeed, regions of ssDNA are frequently detected on the regressed arm of a reversed fork (47). It has been suggested that reversed forks are formed in yeast cells at RFBs in the rDNA (48), and there are accumulating evidence that stalled replication forks are very prone to fork reversal (47,49–51). If fork reversal is a frequent incidence at RFBs even in wild-type cells, it is attractive to think of the MRX complex as a 'protector' of the structure (Figure 9A). On fork reversal, a double-stranded end is exposed, which can be recognized by the MRX complex. Binding of the MRX complex to this end could potentially protect the structure from further processing. Our ChIP data would also be consistent with this hypothesis.

The observed growth defect is identical for *GAL-FOB1 mre11Δ* and *GAL-FOB1* eRFB *mre11Δ* strains. Thus, the ectopically RFBs do not contribute additionally to a growth defect. It is tempting to believe that the growth defect stems from problems arising directly at the RFBs, but we cannot rule out that it originates owing to other problems in the rDNA. Replication in the rDNA is not only challenged by the unidirectional mode of replication but also owing to its repetitive nature, unusual secondary structures that may affect DNA replication (e.g. creating more stalling) are also more likely to be generated in this region. Together, this would create a stronger need for the MRX complex in this region either to suppress fork reversal or protect a reversed fork. Thus, we cannot exclude that the rightward-moving fork in the rDNA encounters problems in the absence of the MRX complex, although this is not the case for the rightward-moving fork in the *ARS606–ARS607* region (Figure 7).

The cellular implications in the rDNA on *FOB1* induction and in the absence of Mre11 are to our surprise

checkpoint blind (Figure 8B), which is in striking contrast to the checkpoint activation arising when forks stall at ectopically placed barriers in the absence of Mre11 (Figure 9B). We believe that it is a structure arising at the ectopic barrier, which is checkpoint activating, as we fail to detect unreplicated DNA in this region, supporting that a fully competent fork emanates from *ARS606*. Opposed to the rDNA and to our surprise, we fail to detect more RPA at this location; however, this is probably due to limitations in our ChIP experiments.

Why is it that abnormal structures at ectopically placed RFBs are checkpoint activating but checkpoint blind in the rDNA? It has been shown that a DSB induced in the rDNA by the endonuclease I-*Sce*I is checkpoint activating; thus, the unique heterochromatic structure found in the rDNA is not enough to suppress a checkpoint response under normal circumstances (52). Furthermore, we can rule out a general function of Mre11 for checkpoint activation in the rDNA, as we can detect checkpoint activation when a DSB is induced by the endonuclease I-*Sce*I in the absence of Mrell (Supplementary Figure S4). However, we considered the idea that overexpression of Fob1 in our Fob-block system could lead to a significant higher level of heterochromatic structure in the rDNA, which may impact checkpoint activation. Indeed, when *SIR2* is deleted, we are able to detect Rad53 activation to the same level as seen in strains with ectopically placed RFBs. Thus, disturbance of a balanced rDNA silencing may adversely affect the checkpoint response. This effect may be direct in that the heterochromatic structure hinders access of checkpoint sensors and thereby suppress the checkpoint response. However, it is also easy to imagine that unbalanced rDNA silencing encumbers proper processing of the DNA at the RFBs into a strong checkpoint activating structure. Another attractive possibility is that *SIR2* in general suppresses checkpoint in the vicinity of RFBs.

Our finding that a *SIR2* deletion restores checkpoint activation points to a significant influence of chromatin structure on checkpoint activation in the rDNA. In line with this, it has been reported that heterochromatin could pose a barrier to the DNA damage response pathway (53–57), and more recent, it was furthermore shown that heterochromatin induced by oncogenic stress restrains DNA damage response (58).

It is reasonable to picture that there is a delicate balance in the rDNA to know whether a checkpoint response is activated. In the Rdna, both replication dependent and independent double strand breaks occur in each cell cycle, which are not checkpoint activating (41), whereas an I-*Sce*I generated DSB causes checkpoint activation [Supplementary Figure S3 and (52)]. Thus, in the rDNA, there may be an inherent way to distinguish between natural or aberrant damage. Alternatively, as RFBs are a natural integrated part of the rDNA, and a hotspot for DSBs, it is attractive to suggest that Sir2 in general suppresses checkpoint activation in the vicinity of the RFBs. Future studies will hopefully uncover the underlying mechanism controlling this phenomenon and unravel whether this is evolutionarily conserved.

SUPPLEMENTRY DATA

Supplementary Data are available at NAR Online: Supplementary Tables 1–3, Supplementary Figures 1–4, Supplementary Methods and Supplementary reference [59]

ACKNOWLEDGEMENTS

The authors thank F. Uhlmann for the gift of *ssc1-73* strain and L. Symington for the *mre11*-H125N allele, and J. Petrini for the Rad50 mutant strains.

FUNDING

Danish Research Counsil [FNU 21-04-0354, FNU 272-07-0366]; Aase og Einar Danielsens Foundation; Augustinus Foundation and Dagmar Marshall Foundation (to L.B.), the Danish Cancer Society (to A.H.A. and L.B.). The Lundbeckfoundation (53/06) (to I.B.B.); the Villum Kann Rasmussen Foundation and the European Research Council (to M.L.). Funding for open access charge: Augustinus Foundation.

Conflict of interest statement. None declared.

REFERENCES

1. Admire,A., Shanks,L., Danzl,N., Wang,M., Weier,U., Stevens,W., Hunt,E. and Weinert,T. (2006) Cycles of chromosome instability are associated with a fragile site and are increased by defects in DNA replication and checkpoint controls in yeast. *Genes Dev.*, **20**, 159–173.
2. Glover,T.W. (2006) Common fragile sites. *Cancer Lett.*, **232**, 4–12.
3. Lambert,S. and Carr,A.M. (2005) Checkpoint responses to replication fork barriers. *Biochimie*, **87**, 591–602.
4. Tourriere,H. and Pasero,P. (2007) Maintenance of fork integrity at damaged DNA and natural pause sites. *DNA Repair (Amst.)*, **6**, 900–913.
5. Brewer,B.J., Lockshon,D. and Fangman,W.L. (1992) The arrest of replication forks in the rDNA of yeast occurs independently of transcription. *Cell*, **71**, 267–276.
6. Kobayashi,T. (2011) Regulation of ribosomal RNA gene copy number and its role in modulating genome integrity and evolutionary adaptability in yeast. *Cell Mol. Life Sci.*, **68**, 1395–1403.
7. Dalgaard,J.Z. and Klar,A.J. (2000) swi1 and swi3 perform imprinting, pausing, and termination of DNA replication in S. pombe. *Cell*, **102**, 745–751.
8. Katou,Y., Kanoh,Y., Bando,M., Noguchi,H., Tanaka,H., Ashikari,T., Sugimoto,K. and Shirahige,K. (2003) S-phase checkpoint proteins Tof1 and Mrc1 form a stable replication-pausing complex. *Nature*, **424**, 1078–1083.
9. Desany,B.A., Alcasabas,A.A., Bachant,J.B. and Elledge,S.J. (1998) Recovery from DNA replicational stress is the essential function of the S-phase checkpoint pathway. *Genes Dev.*, **12**, 2956–2970.
10. Cobb,J.A., Bjergbaek,L., Shimada,K., Frei,C. and Gasser,S.M. (2003) DNA polymerase stabilization at stalled replication forks requires Mec1 and the RecQ helicase Sgs1. *EMBO J.*, **22**, 4325–4336.
11. Lopes,M., Cotta-Ramusino,C., Pellicioli,A., Liberi,G., Plevani,P., Muzi-Falconi,M., Newlon,C.S. and Foiani,M. (2001) The DNA replication checkpoint response stabilizes stalled replication forks. *Nature*, **412**, 557–561.
12. Tercero,J.A., Longhese,M.P. and Diffley,J.F. (2003) A central role for DNA replication forks in checkpoint activation and response. *Mol. Cell*, **11**, 1323–1336.

13. Tercero,J.A. and Diffley,J.F. (2001) Regulation of DNA replication fork progression through damaged DNA by the Mec1/Rad53 checkpoint. *Nature*, **412**, 553–557.
14. Calzada,A., Hodgson,B., Kanemaki,M., Bueno,A. and Labib,K. (2005) Molecular anatomy and regulation of a stable replisome at a paused eukaryotic DNA replication fork. *Genes Dev.*, **19**, 1905–1919.
15. Lambert,S., Watson,A., Sheedy,D.M., Martin,B. and Carr,A.M. (2005) Gross chromosomal rearrangements and elevated recombination at an inducible site-specific replication fork barrier. *Cell*, **121**, 689–702.
16. Ahn,J.S., Osman,F. and Whitby,M.C. (2005) Replication fork blockage by RTS1 at an ectopic site promotes recombination in fission yeast. *EMBO J.*, **24**, 2011–2023.
17. Bidnenko,V., Ehrlich,S.D. and Michel,B. (2002) Replication fork collapse at replication terminator sequences. *EMBO J.*, **21**, 3898–3907.
18. Courcelle,J., Donaldson,J.R., Chow,K.H. and Courcelle,C.T. (2003) DNA damage-induced replication fork regression and processing in *Escherichia coli*. *Science*, **299**, 1064–1067.
19. Lambert,S., Mizuno,K., Blaisonneau,J., Martineau,S., Chanet,R., Freon,K., Murray,J.M., Carr,A.M. and Baldacci,G. (2010) Homologous recombination restarts blocked replication forks at the expense of genome rearrangements by template exchange. *Mol. Cell*, **39**, 346–359.
20. Mizuno,K., Lambert,S., Baldacci,G., Murray,J.M. and Carr,A.M. (2009) Nearby inverted repeats fuse to generate acentric and dicentric palindromic chromosomes by a replication template exchange mechanism. *Genes Dev.*, **23**, 2876–2886.
21. Nielsen,I., Bentsen,I.B., Lisby,M., Hansen,S., Mundbjerg,K., Andersen,A.H. and Bjergbaek,L. (2009) A Flp-nick system to study repair of a single protein-bound nick *in vivo*. *Nat. Methods*, **6**, 753–757.
22. Frei,C. and Gasser,S.M. (2000) The yeast Sgs1p helicase acts upstream of Rad53p in the DNA replication checkpoint and colocalizes with Rad53p in S-phase-specific foci. *Genes Dev.*, **14**, 81–96.
23. Wu,J.R. and Gilbert,D.M. (1995) Rapid DNA preparation for 2D gel analysis of replication intermediates. *Nucleic Acids Res.*, **23**, 3997–3998.
24. Huberman,J.A., Spotila,L.D., Nawotka,K.A., el-Assouli,S.M. and Davis,L.R. (1987) The in vivo replication origin of the yeast 2 microns plasmid. *Cell*, **51**, 473–481.
25. Maringele,L. and Lydall,D. (2006) Pulsed-field gel electrophoresis of budding yeast chromosomes. *Methods Mol. Biol.*, **313**, 65–73.
26. Pellicioli,A., Lucca,C., Liberi,G., Marini,F., Lopes,M., Plevani,P., Romano,A., Di Fiore,P.P. and Foiani,M. (1999) Activation of Rad53 kinase in response to DNA damage and its effect in modulating phosphorylation of the lagging strand DNA polymerase. *EMBO J.*, **18**, 6561–6572.
27. Zou,H. and Rothstein,R. (1997) Holliday junctions accumulate in replication mutants via a RecA homolog-independent mechanism. *Cell*, **90**, 87–96.
28. Burkhalter,M.D. and Sogo,J.M. (2004) rDNA enhancer affects replication initiation and mitotic recombination: Fob1 mediates nucleolytic processing independently of replication. *Mol. Cell*, **15**, 409–421.
29. Straight,A.F., Shou,W., Dowd,G.J., Turck,C.W., Deshaies,R.J., Johnson,A.D. and Moazed,D. (1999) Net1, a Sir2-associated nucleolar protein required for rDNA silencing and nucleolar integrity. *Cell*, **97**, 245–256.
30. Huang,J. and Moazed,D. (2003) Association of the RENT complex with nontranscribed and coding regions of rDNA and a regional requirement for the replication fork block protein Fob1 in rDNA silencing. *Genes Dev.*, **17**, 2162–2176.
31. Mimitou,E.P. and Symington,L.S. (2008) Sae2, Exo1 and Sgs1 collaborate in DNA double-strand break processing. *Nature*, **455**, 770–774.
32. Shim,E.Y., Chung,W.H., Nicolette,M.L., Zhang,Y., Davis,M., Zhu,Z., Paull,T.T., Ira,G. and Lee,S.E. (2010) Saccharomyces cerevisiae Mre11/Rad50/Xrs2 and Ku proteins regulate association of Exo1 and Dna2 with DNA breaks. *EMBO J.*, **29**, 3370–3380.
33. Zhu,Z., Chung,W.H., Shim,E.Y., Lee,S.E. and Ira,G. (2008) Sgs1 helicase and two nucleases Dna2 and Exo1 resect DNA double-strand break ends. *Cell*, **134**, 981–994.
34. Cejka,P., Cannavo,E., Polaczek,P., Masuda-Sasa,T., Pokharel,S., Campbell,J.L. and Kowalczykowski,S.C. (2010) DNA end resection by Dna2-Sgs1-RPA and its stimulation by Top3-Rmi1 and Mre11-Rad50-Xrs2. *Nature*, **467**, 112–116.
35. Niu,H., Chung,W.H., Zhu,Z., Kwon,Y., Zhao,W., Chi,P., Prakash,R., Seong,C., Liu,D., Lu,L. *et al.* (2010) Mechanism of the ATP-dependent DNA end-resection machinery from *Saccharomyces cerevisiae*. *Nature*, **467**, 108–111.
36. Bressan,D.A., Baxter,B.K. and Petrini,J.H. (1999) The Mre11-Rad50-Xrs2 protein complex facilitates homologous recombination-based double-strand break repair in Saccharomyces cerevisiae. *Mol. Cell Biol.*, **19**, 7681–7687.
37. Mimitou,E.P. and Symington,L.S. (2010) Ku prevents Exo1 and Sgs1-dependent resection of DNA ends in the absence of a functional MRX complex or Sae2. *EMBO J.*, **29**, 3358–3369.
38. Hohl,M., Kwon,Y., Galvan,S.M., Xue,X., Tous,C., Aguilera,A., Sung,P. and Petrini,J.H. (2011) The Rad50 coiled-coil domain is indispensable for Mre11 complex functions. *Nat. Struct. Mol. Biol.*, **18**, 1124–1131.
39. Tittel-Elmer,M., Alabert,C., Pasero,P. and Cobb,J.A. (2009) The MRX complex stabilizes the replisome independently of the S phase checkpoint during replication stress. *EMBO J.*, **28**, 1142–1156.
40. Weitao,T., Budd,M., Hoopes,L.L. and Campbell,J.L. (2003) Dna2 helicase/nuclease causes replicative fork stalling and double-strand breaks in the ribosomal DNA of Saccharomyces cerevisiae. *J. Biol. Chem.*, **278**, 22513–22522.
41. Fritsch,O., Burkhalter,M.D., Kais,S., Sogo,J.M. and Schar,P. (2010) DNA ligase 4 stabilizes the ribosomal DNA array upon fork collapse at the replication fork barrier. *DNA Repair (Amst.)*, **9**, 879–888.
42. Weitao,T., Budd,M. and Campbell,J.L. (2003) Evidence that yeast SGS1, DNA2, SRS2, and FOB1 interact to maintain rDNA stability. *Mutat. Res.*, **532**, 157–172.
43. Uhlmann,F., Lottspeich,F. and Nasmyth,K. (1999) Sister-chromatid separation at anaphase onset is promoted by cleavage of the cohesin subunit Scc1. *Nature*, **400**, 37–42.
44. Torres,J.Z., Schnakenberg,S.L. and Zakian,V.A. (2004) Saccharomyces cerevisiae Rrm3p DNA helicase promotes genome integrity by preventing replication fork stalling: viability of rrm3 cells requires the intra-S-phase checkpoint and fork restart activities. *Mol. Cell. Biol.*, **24**, 3198–3212.
45. Hopfner,K.P., Craig,L., Moncalian,G., Zinkel,R.A., Usui,T., Owen,B.A., Karcher,A., Henderson,B., Bodmer,J.L., McMurray,C.T. *et al.* (2002) The Rad50 zinc-hook is a structure joining Mre11 complexes in DNA recombination and repair. *Nature*, **418**, 562–566.
46. Doksani,Y., Bermejo,R., Fiorani,S., Haber,J.E. and Foiani,M. (2009) Replicon dynamics, dormant origin firing, and terminal fork integrity after double-strand break formation. *Cell*, **137**, 247–258.
47. Ray Chaudhuri,A., Hashimoto,Y., Herrador,R., Neelsen,K.J., Fachinetti,D., Bermejo,R., Cocito,A., Costanzo,V. and Lopes,M. (2012) Topoisomerase I poisoning results in PARP-mediated replication fork reversal. *Nat. Struct. Mol. Biol.*, **19**, 417–423.
48. Defossez,P.A., Prusty,R., Kaeberlein,M., Lin,S.J., Ferrigno,P., Silver,P.A., Keil,R.L. and Guarente,L. (1999) Elimination of replication block protein Fob1 extends the life span of yeast mother cells. *Mol. Cell*, **3**, 447–455.
49. Atkinson,J. and McGlynn,P. (2009) Replication fork reversal and the maintenance of genome stability. *Nucleic Acids Res.*, **37**, 3475–3492.
50. Postow,L., Crisona,N.J., Peter,B.J., Hardy,C.D. and Cozzarelli,N.R. (2001) Topological challenges to DNA replication: conformations at the fork. *Proc. Natl Acad. Sci. USA*, **98**, 8219–8226.
51. Postow,L., Ullsperger,C., Keller,R.W., Bustamante,C., Vologodskii,A.V. and Cozzarelli,N.R. (2001) Positive torsional strain causes the formation of a four-way junction at replication forks. *J. Biol. Chem.*, **276**, 2790–2796.

52. Torres-Rosell,J., De Piccoli,G., Cordon-Preciado,V., Farmer,S., Jarmuz,A., Machin,F., Pasero,P., Lisby,M., Haber,J.E. and Aragon,L. (2007) Anaphase onset before complete DNA replication with intact checkpoint responses. *Science*, **315**, 1411–1415.
53. Goodarzi,A.A., Noon,A.T., Deckbar,D., Ziv,Y., Shiloh,Y., Lobrich,M. and Jeggo,P.A. (2008) ATM signaling facilitates repair of DNA double-strand breaks associated with heterochromatin. *Mol. Cell.*, **31**, 167–177.
54. Kim,J.A., Kruhlak,M., Dotiwala,F., Nussenzweig,A. and Haber,J.E. (2007) Heterochromatin is refractory to gamma-H2AX modification in yeast and mammals. *J. Cell Biol.*, **178**, 209–218.
55. Murga,M., Jaco,I., Fan,Y., Soria,R., Martinez-Pastor,B., Cuadrado,M., Yang,S.M., Blasco,M.A., Skoultchi,A.I. and Fernandez-Capetillo,O. (2007) Global chromatin compaction limits the strength of the DNA damage response. *J. Cell Biol.*, **178**, 1101–1108.
56. Noon,A.T., Shibata,A., Rief,N., Lobrich,M., Stewart,G.S., Jeggo,P.A. and Goodarzi,A.A. (2010) 53BP1-dependent robust localized KAP-1 phosphorylation is essential for heterochromatic DNA double-strand break repair. *Nat. Cell Biol.*, **12**, 177–184.
57. Ziv,Y., Bielopolski,D., Galanty,Y., Lukas,C., Taya,Y., Schultz,D.C., Lukas,J., Bekker-Jensen,S., Bartek,J. and Shiloh,Y. (2006) Chromatin relaxation in response to DNA double–strand breaks is modulated by a novel ATM- and KAP-1 dependent pathway. *Nat. Cell Biol.*, **8**, 870–876.
58. Di Micco,R., Sulli,G., Dobreva,M., Liontos,M., Botrugno,O.A., Gargiulo,G., dal Zuffo,R., Matti,V., d'Ario,G., Montani,E. *et al.* (2011) Interplay between oncogene-induced DNA damage response and heterochromatin in senescence and cancer. *Nat. Cell Biol.*, **13**, 292–302.
59. Lisby,M. and Rothstein,R. (2008) Differential regulation of the cellular response to DNA double strand breaks in G1. *Mol. Cell*, **30**, 73–85.